Eng. Sci., 2021, **15**, 138–147

Engineered Science

DOI: https://dx.doi.org/10.30919/es8d500

Fabrication and Characterization of an Ultrasensitive Humidity Sensor Based on Chalcogenide Glassy Alloy Thin Films

Surabhi Mishra,[1] Priyanka Chaudhary,[2] B. C. Yadav,[2] Ahmad Umar,[3,*] Pooja Lohia[4] and D. K. Dwivedi[1,*]

Abstract

Herein, a humidity sensor with enhanced sensitivity based on newly prepared chalcogenide glassy alloys thin films was fabricated. Two different chalcogenide glassy alloys, *i.e.* $(Ge_{11.5}Te_{12.5}Se_{67.5})_{100}$ and $(Ge_{11.5}Te_{12.5}Se_{67.5})_{90}Sb_{10}$ were prepared, characterized and finally used to fabricate impedance-based humidity sensors at different frequencies. The fabricated humidity sensors based on $(Ge_{11.5}Te_{12.5}Se_{67.5})_{100}$ and $(Ge_{11.5}Te_{12.5}Se_{67.5})_{90}Sb_{10}$ thin films exhibited high sensitivities of ~8.522 MΩ/%RH and 9.280 MΩ/%RH, respectively. Compared with other humidity sensors based on metal oxides and other nanocomposites, the fabricated humidity sensors based on $(Ge_{11.5}Te_{12.5}Se_{67.5})_{100}$ and $(Ge_{11.5}Te_{12.5}Se_{67.5})_{90}Sb_{10}$ thin films demonstrated better sensing properties. Moreover, the fabricated sensors revealed faster response and recovery times. The response and recovery times for the fabricated humidity sensor based on $(Ge_{11.5}Te_{12.5}Se_{67.5})_{100}$ were 30s and 44s, respectively while the $(Ge_{11.5}Te_{12.5}Se_{67.5})_{90}Sb_{10}$ chalcogenide thin film-based humidity sensor shows 28 s response and 34 s recovery times. Based on the perceived results, it can be concluded that the newly prepared chalcogenide glassy alloys thin films based on $(Ge_{11.5}Te_{12.5}Se_{67.5})_{100}$ and $(Ge_{11.5}Te_{12.5}Se_{67.5})_{90}Sb_{10}$ are promising materials to fabricate high-sensitive humidity sensors for variety of applications.

Keywords: Chalcogenide glasses; Humidity sensor; Sensitivity; Sensor response.
Received: 3 July 2021; Accepted: 1 August 2021.
Article type: Research article.

1. Introduction

The most essential component of life on earth is water which exists in two different forms viz. moisture which is liquid (condensed) form and humidity which refers to gaseous phase of water.[1-2] The highly reactive dipolar molecules of water gets evaporated or condensed from surface even in slight variation of environmental temperature.[3] Hence, humidity has control on various environmental phenomena. Control and measurement of humidity in the environment have great importance in agricultural productions, industrial processes, and research experiments.[4] Based on various mechanisms like resistance, capacitance different types of sensors have been developed.[5-7] The everfast progress in science and technology now a day requires humidity sensors having better sensitivity, faster response, wider sensing range, lower cost, and shorter recovery time. Much efforts have been done to prepare highly sensitive materials and novel devices for solving such issues.[8,9]

Chalcogenide glasses (ChG) are used in a wide range of technological applications because of their excellent properties such as optical transparency, large glass-forming ability, high chemical durability and so on.[10] In comparison to other crystalline chalcogenide glasses have properties like easier shaping, stability over time that makes it an interesting candidate for sensor application.[11] The high transmission of chalcogenides glasses in infrared region makes them suitable candidates for active and passive IR devices.[12] Among all chalcogenide glasses studied earlier, Ge-Te-Se, Ge-Te-As-Se, As-Se, Ge-Se-I are most promising materials which are widely used for mid IR sensor applications.[13] Different types of sensors like chemical sensor, radiation sensor, gas sensor,

[1] *Amorphous Semiconductor Research Lab, Department of Physics and Material Science, Madan Mohan Malaviya University of Technology, Gorakhpur-273010, India.*
[2] *Nanomaterials and Sensors Research Laboratory, Department of Physics, Babasaheb Bhimrao Ambedkar University, Lucknow-226025, Utter Pradesh, India.*
[3] *Department of Chemistry, Faculty of Science and Arts and Promising Centre for Sensors and Electronic Devices (PCSED), Najran University, Najran-11001, Kingdom of Saudi Arabia.*
[4] *Department of Electronics and Communication Engineering, Madan Mohan Malaviya University of Technology, Gorakhpur-273010, India.*
**Email:* ahmadumar786@gmail.com (A. Umar);
todkdwivedi@gmail.com (D. Dwivedi.)

biological sensor *etc* are already studied for chalcogenide glass membranes. For example, Yoo *et al*. had studied As_2S_3 as respiratory sensor that can operate in low-temperature range of 7 to 127 ˚C.[14] Chalcogenide glasses also have property to transform photoelectric phenomenon and could create junction once contacted with metal, thus can be utilized as image sensors.[15,16] Mitkova *et al*. have studied Ge-Se-Ag as radiation sensor because of its flexible atomic structure and radiation induced phenomenon.[17] The graphene based three-layer sensor was studied by Sharma *et al.* for testing hemoglobin concentration in blood of human using chalcogenide optical fiber as $As_{40}S_{60}$ for core and $Ge_{20}Ga_5Sb_{10}S_{65}$ for cladding.[18]

Recently, chalcogenide glasses are also used as membrane materials for the fabrication of chemical sensors, gas sensors, multi sensors and micro-sensors systems.[19] Because of the chemical stability, better redox performance, better selectivity, reproducibility and longer life time, the chalcogenide glasses are one of the important and fascinating materials for various sensor applications. Legin *et al*. demonstrated the fabrication and characterization of chalcogenide glasses based chemical sensors for the efficient determination of chromium (VI), iorn (III), copper (II), cadmium, mercury, and lead.[20] Chalcogenide glasses based thin film ion selective chemical sensor for the determination of heavy metal ions was developed and reported by Tomova *et al*.[21] Mourzina *et al*. reported the chalcogenide glasses thin film with different systems, *i.e.* Tl–Ag–As–I–S, Ag–I–As–Se, Ag–I–As–S, Cd–Ag–As–I–S, Cu–Ag–As–Se–Te, and Ag–As–Te–Se based micro-sensors for the selective determination of copper, cadmium and thallium.[22] Solid state electrochemical sensor based on chalcogenide glasses for the selective determination of Cu(II) and Pb(II) ions was reported by A. E. Owen.[23] Complex $(As_2S_3)_{100-x}(AgI)_x$ chalcogenide glasses-based gas sensors for the determination of various gases such as water, methanol, isopropanol and acetone were fabricated by Kolev *et al*. and it was observed that the made-up gas sensor exhibited highest sensitivity towards acetone gas compared to other examined gases.[24] Even though chalcogenide glasses are widely used for variety of applications, but to the best of our understanding, these materials are rarely used for humidity sensing applications. Moreover, the humidity sensors also encountered with several other glitches which include their long response and recovery times, low-sensitivity, and detection range in the narrow region. Thus, to overcome such problems, there is a serious need to develop a new humidity sensor which possess high sensitivity, low response and recovery times with a reasonable detection range.

Herein, we present the fabrication and characterization of two new chalcogenide glassy alloys, *i.e.* $(Ge_{11.5}Te_{12.5}Se_{67.5})_{100}$ and $(Ge_{11.5}Te_{12.5}Se_{67.5})_{90}Sb_{10}$ based humidity sensors. To the best of our understanding, this is first ever report on the fabrication of humidity sensor based on $(Ge_{11.5}Te_{12.5}Se_{67.5})_{100-x}Sb_x$ chalcogenide thin films. The detailed characteristics of the fabricated humidity sensors were studied and presented in this paper.

2. Experimental section

2.1. Bulk material

The bulk samples of $(Ge_{11.5}Te_{12.5}Se_{67.5})_{90}Sb_{10}$ and $(Ge_{11.5}Te_{12.5}Se_{67.5})_{100}$ glassy alloys were formulated by the standard melt-quenching technique as reported earlier.[25] In summary, precise proportions of high purity (99.999%) metallic powders of germanium (Ge), Tellurium (Te), Antimony (Sb) and Selenium (Se), were mixed well, in accordance to the atomic weight percentages, and transferred in ampoules and sealed under high vacuum, *i.e.* 10^{-6} Pa. The sealed ampoule was then transferred to a special furnace and heated at 900 °C with the heating rate of 4°C/min for 10 h. Continuous rotation of ampoule was done during the reaction in order to maintain the homogeneity of the reactant powders. After the desired reaction time, the ampoule was melt-quenched in ice cool water for solidification. Fig. 1 exhibits the typical synthesis process of prepared $(Ge_{11.5}Se_{67.5}Te_{12.5})_{100}$ chalcogenide bulk material.

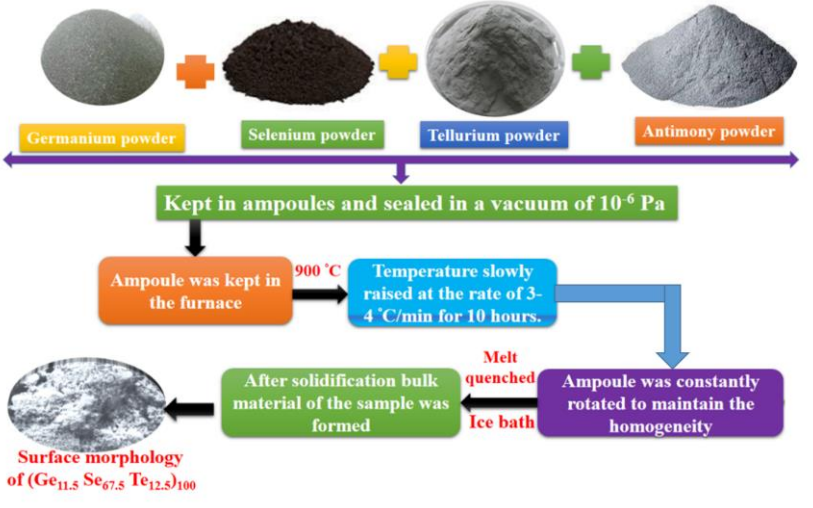

Fig. 1 Typical synthesis process of $(Ge_{11.5}\ Se_{67.5}\ Te_{12.5})_{100}$ chalcogenide material.

2.2. Preparation of sensing membrane

Thin films of prepared chalcogenide material were obtained with vacuum thermal evaporation unit (vacuum equipment company, Noida, India) inbuilt with quartz crystal monitor. The glass substrate was cleaned with methanol and acetone, sequentially in order to remove impurities and then dried in the laboratory oven for drying. After cleansing, the substrate was placed in the stand under the vacuum thermal evaporation unit. The bulk sample of $(Ge_{11.5}Te_{12.5}Se_{67.5})_{100}$ and $(Ge_{11.5}Te_{12.5}Se_{67.5})_{90}Sb_{10}$ was crushed in the mortar to obtain a fine powder which was used as a source material for the deposition of thin film. A clean glass slide was used as substrate for the deposition of chalcogenides. Thermal evaporator was used to deposit the chalcogenides over the glass substrates. For the thin film growth, the fine powder was put in the molybdenum boat and glass substrate was placed above it in the thermal evaporator chamber. After this arrangement, the chamber pressure was down to 10^{-6} Pa. During the deposition, the substrate temperature was 100 °C. The thickness of the thin film was measured by Quartz Crystal Digital Thickness Monitor DTM-200.

2.3 Sensing setup

The typical humidity sensing set up consists of a glass chamber to obtain a controlled humid atmosphere. A hygrometer (model: HTC -1) was used to measure the level of humidity in %RH. Saturated K_2SO_4 was used as a humidifier and saturated KOH for the dehumidifier in the humidity chamber. For measuring impedance Wayne Kerr Precision Component Analyzer, 6440B was used in the sensing setup that gives impedance in range 0.01 mΩ to > 2 GΩ. An impedance analyzer with two copper wires was connected to the sensing element that was fixed with 1 mm width of silver electrodes with 3 mm spacing.

2.4. Characterization techniques

Various characterization techniques have been used to investigate the structural and optical characteristics of the chalcogenide sensing element. X-ray diffraction (XRD: Rigaku mini flex 600) using Cu-Kα radiation (λ=1.54 Å) with step size 0.02º in the range of 10º to 80º diffraction angle was used to study the crystallographic and formation phases of the sensing films. Scanning electron microscopy (SEM: Zeiss EVO40) was used to study the morphologies of the prepared thin films. The optical properties were examined by UV-Vis absorption spectrophotometer (model: UV5704SS) in the range of 300 to 1000 nm.

3. Results and discussions

3.1 Characterizations and properties of $(Ge_{11.5}Te_{12.5}Se_{67.5})_{90}Sb_{10}$ and $(Ge_{11.5}Te_{12.5}Se_{67.5})_{100}$ chalcogenide glasses

Fig. 2 exhibits the typical XRD patterns of $(Ge_{11.5}Te_{12.5}Se_{67.5})_{90}Sb_{10}$ and $(Ge_{11.5}Te_{12.5}Se_{67.5})_{100}$ chalcogenide glasses. The observed diffraction patterns exhibited two broad halos which confirms the amorphous network and long-range structural disorder in the prepared chalcogenide glasses. The result shows that all samples were amorphous regardless of change in the chemical composition of the samples.

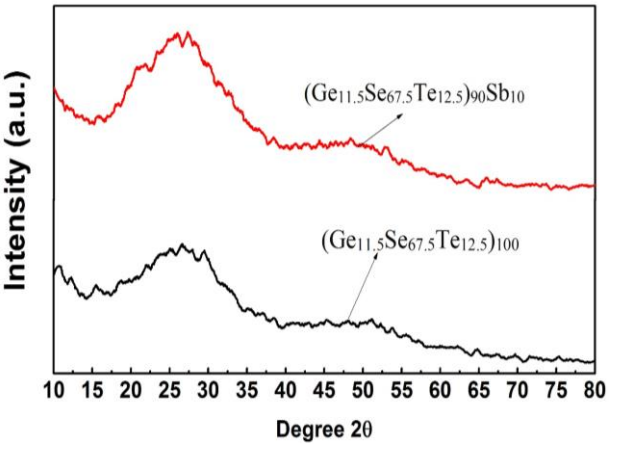

Fig. 2 XRD patterns of $(Ge_{11.5}Te_{12.5}Se_{67.5})_{90}Sb_{10}$ and $(Ge_{11.5}Te_{12.5}Se_{67.5})_{100}$ chalcogenide glasses.

Figs. 3(a-b) demonstrate the surface morphologies of the $(Ge_{11.5}Te_{12.5}Se_{67.5})_{100}$ and $(Ge_{11.5}Te_{12.5}Se_{67.5})_{90}Sb_{10}$ chalcogenide glasses which are coded as X-0 and X-10, respectively. The inhomogeneity of the powder and the glassy nature of the material can be seen from the SEM analysis. It is obvious from the morphology that due to the glassy nature we have not observed any crystalline-like nature which is also confirmed from the XRD analysis. The performance of humidity sensors is not only based on the morphological characteristics of the deposited films but also the metals such as germanium, tellurium, selenium, and antimony play a major role in the humidity sensing performance. Germanium has moderately wide, indirect energy gap (0.7 eV) and also have complex band edge structure that makes the, important candidate for IR applications. Selenium is considered as a suitable material for the IR devices due to its exceptional properties like superconductivity, piezoelectricity, catalytic activities, anisotropy of thermo-conductivity, thermoelectricity, and nonlinear optical responses.

Tellurium based glasses have transparency to infrared radiation which increases towards smaller wavenumbers. Antimony increases the sensitivity because of its metallic properties. Since germanium, tellurium, selenium, and antimony are the metals which have electropositive nature. Presence of these metal ions acts as an active site for the interaction with water molecules and responsible for formation of initial chemisorbed layer.

The elemental composition of the prepared films was examined by energy dispersive spectroscopy (EDS) and results are demonstrated in Figs. 3(c-d). The observed EDS spectra of the prepared samples confirmed that all constituent elements are present in the same stoichiometry following theoretical composition in the sample prepared by

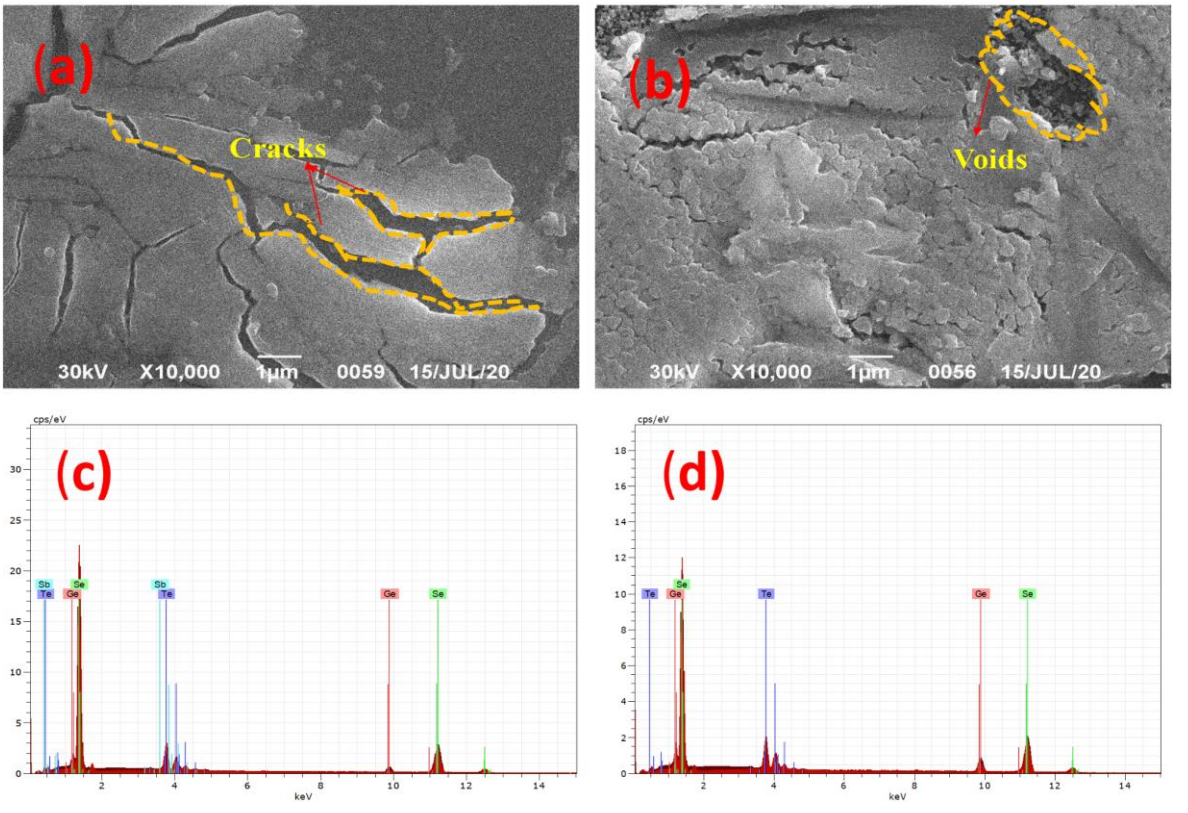

Fig. 3 (a) SEM micrograph of $(Ge_{11.5}\ Se_{67.5}\ Te_{12.5})_{100}$ (b) $(Ge_{11.5}\ Se_{67.5}\ Te_{12.5})_{90}\ Sb_{10}$ chalcogenide glassy alloy (c) EDX spectra of $(Ge_{11.5}\ Se_{67.5}\ Te_{12.5})_{100}$, and (d) $(Ge_{11.5}\ Se_{67.5}\ Te_{12.5})_{90}\ Sb_{10}$ chalcogenide glassy alloy.

Table 1. EDS data of $(Ge_{11.5}\ Se_{67.5}\ Te_{12.5})_{100}$ and $(Ge_{11.5}\ Se_{67.5}\ Te_{12.5})_{90}Sb_{10}$ chalcogenide glassy alloy.

Composition	Germanium wt %	Selenium wt %	Tellurium wt%	Antimony wt%
x=0	2.40	66.10	31.49	0.00
x=10	2.01	66.73	29.06	2.20

melt quench technique.[26] The quantitative results are listed in Table 1 that shows atomic percentage of prepared composition is nearly equal to required stoichiometry of the materials.

Figs. 4 and 5 shows the absorbance spectra with its corresponding Tauc plot for prepared $(Ge_{11.5}Te_{12.5}Se_{67.5})_{100}$ and $(Ge_{11.5}Te_{12.5}Se_{67.5})_{90}Sb_{10}$ chalcogenide sensing elements. It is clear from the observed absorbance spectra that our sensing element can exhibit absorption in the wavelength range of 300-1000 nm. Insets of Figs. 4 and 5 exhibit the change in optical absorption coefficient (α) with respect to photon energy (hν) which was calculated from absorbance and wavelength data. For obtaining the value of optical bandgap (Eg) of prepared sensing material we have used the following relation:[25]

$$E_g = h\nu - (\alpha h\nu)^{\frac{1}{n}} \quad (1)$$

where ν represents transition frequency and n defines the characteristics of band transition. The band transition is called direct and indirect allowed transition for n=1/2 and n=2 respectively while n=3/2 and n=3 correspond to direct and indirect forbidden transitions respectively. In our case the best fit for the curve comes from n=1/2 hence there is direct allowed transition in the prepared chalcogenide sensing element. The optical bandgap was obtained by extrapolating the graph at hν→0 which is 1.45 eV for $(Ge_{11.5}Te_{12.5}Se_{67.5})_{100}$ and 1.56 eV for $(Ge_{11.5}Te_{12.5}Se_{67.5})_{90}Sb_{10}$ that means the addition of Sb increases the bandgap of sensing elements.[27]

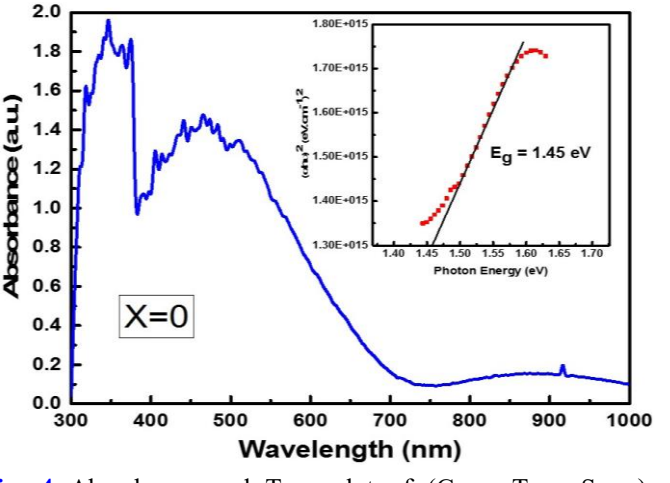

Fig. 4 Absorbance and Tauc plot of $(Ge_{11.5}\ Te_{12.5}\ Se_{67.5})_{100}$ chalcogenide sensing element.

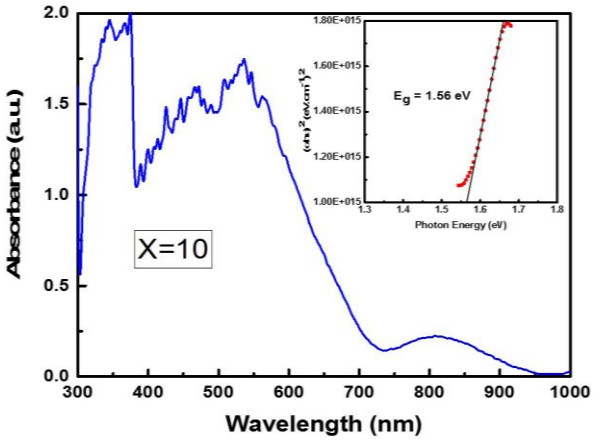

Fig. 5 Absorbance and Tauc plot of $(Ge_{11.5}\ Te_{12.5}\ Se_{67.5})_{90}Sb_{10}$ chalcogenide sensing element.

3.2 Humidity sensing applications of $(Ge_{11.5}Te_{12.5}Se_{67.5})_{90}Sb_{10}$ and $(Ge_{11.5}Te_{12.5}Se_{67.5})_{100}$ chalcogenide glasses

Figs. 6(a-b) and Figs. 7(a-b) show the variation of impedance corresponding with the relative humidity and the impedance for increasing and decreasing mode at a wide frequency range *i.e.* from 10^2-10^5 Hz. It should be noted that the impedance value decreases at a given frequency with an increase in %RH, but increases with the decrease in frequency.[28,29] As per the nature of the curve of Figs. 6(a) and Fig. 7(a) for frequency 100 Hz, it has been divided into three regions 10-25 %RH, 25-50 %RH, and 50-95 %RH. The corresponding sensitivities of $(Ge_{11.5}Te_{12.5}Se_{67.5})_{100}$ chalcogenide sensing element was found as 13.865 MΩ/%RH, 11.220 MΩ/%RH and 0.351 MΩ/%RH at room temperature. For the entire range of %RH, the observed average sensitivity was ~8.522 MΩ/%RH while for $(Ge_{11.5}Te_{12.5}Se_{67.5})_{90}Sb_{10}$ sensitivities in the different region was found to be 15.565 MΩ/%RH, 11.880 and 0.426 MΩ/%RH at room temperature and average sensitivity of this sample in the entire range of %RH was observed 9.280 MΩ/%RH.

Other curves for frequencies 10^3,10^4 and 10^5 Hz show a similar nature with the increasing sensitivity. The minimum sensitivity of $(Ge_{11.5}Te_{12.5}Se_{67.5})_{100}$ was found as 0.019 MW/%RH at 10^5 Hz while after adding antimony the minimum sensitivity was 0.021 MW/%RH at 10^5 Hz.

The sensitivity increases with the inclusion of Sb in the matric, which can be attributed to the large number of water molecules adsorbed on the surface due to the change in the structure, which increases the sample's conductivity and hence the sensitivity increases.[30,31]

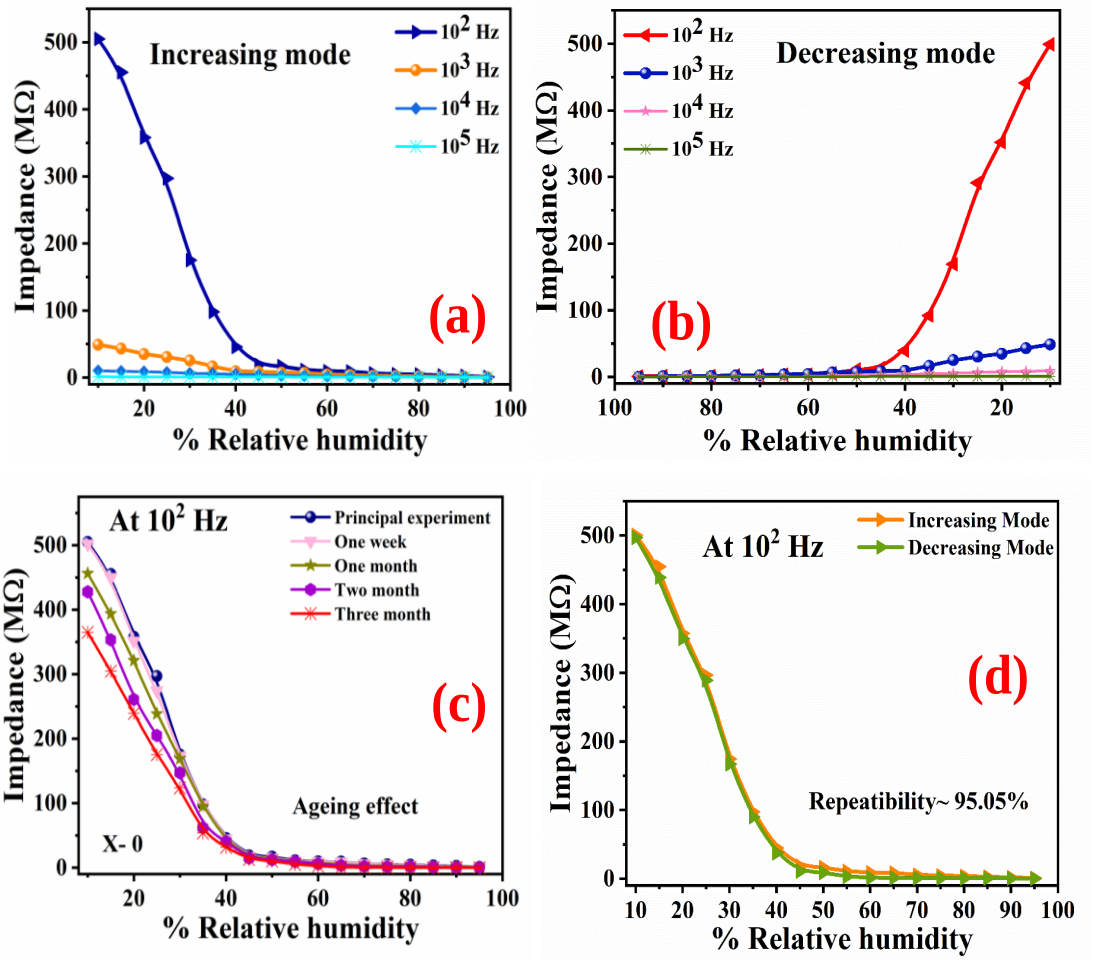

Fig. 6 Variation of output power with %RH for observing (a) sensitivity in increasing mode (b) sensitivity in decreasing mode (c) ageing effect (d) repeatability of $(Ge_{11.5}\ Te_{12.5}\ Se_{67.5})_{100}$ chalcogenide sensing element.

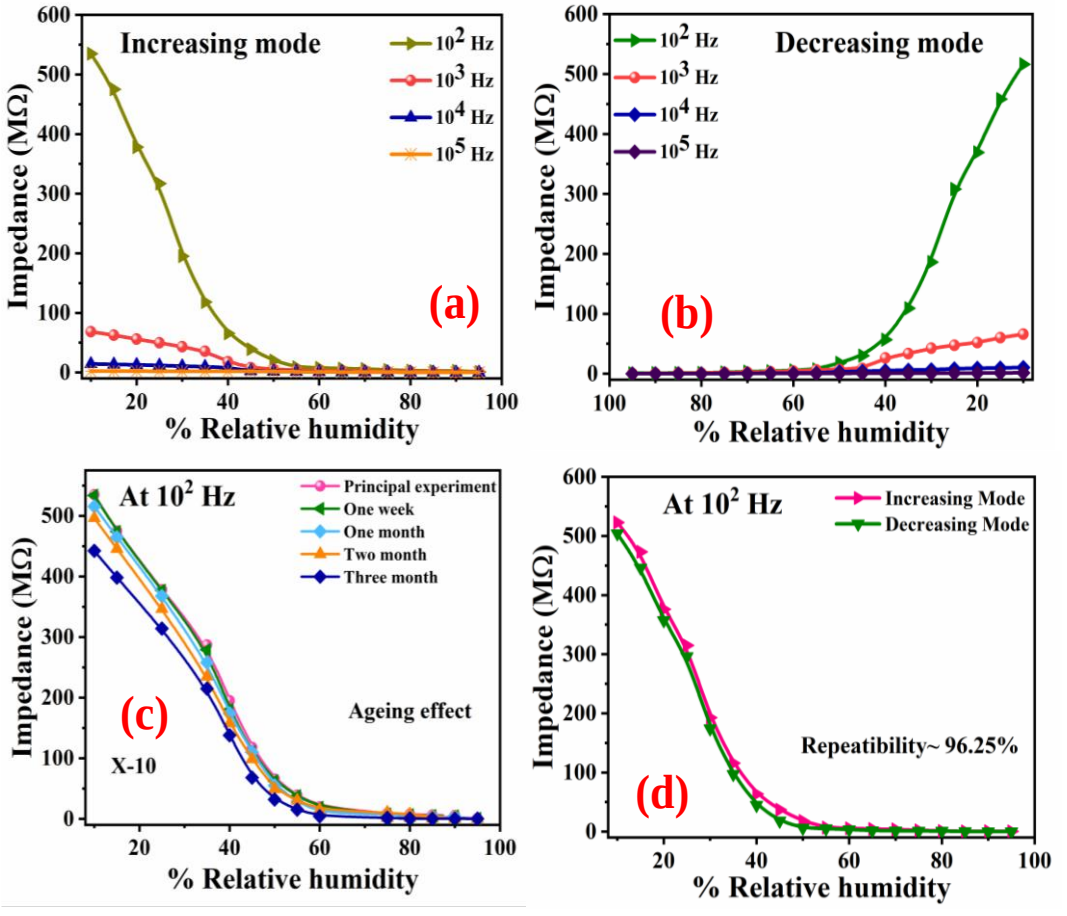

Fig. 7 Variation of output power with %RH for observing (a) sensitivity in increasing mode (b) sensitivity in decreasing mode (c) ageing effect (d) repeatability of $(Ge_{11.5}\ Te_{12.5}\ Se_{67.5})_{90}\ Sb_{10}$ chalcogenide sensing element.

The sensitivity of sensor was calculated from the following formula: [32]

$$S = \frac{Final\ impedance - Initial\ Impedance}{\{\text{Final \%RH} - \text{initial \%RH}\}}\ \text{MΩ/\%RH} \quad (2)$$

Figs. 6(a, b) and Figs. 7(a, b) depict the variations of impedance with increasing and decreasing %RH *i.e.* during the adsorption and desorption of moisture at frequency 100Hz. The repeatability of $(Ge_{11.5}Te_{12.5}Se_{67.5})_{100}$ and $(Ge_{11.5}Te_{12.5}Se_{67.5})_{90}Sb_{10}$ chalcogenide sensing element was calculated as 95.05% and 96.25% respectively as shown in Fig 6(d) and Fig. 7(d), respectively.

The chalcogenides material shows the outstanding humidity sensing properties with good response and recovery time. Because of the high surface to volume ratio, the absorption and desorption capacity also increases and the material is dominant for the interaction between the material and water molecules which is responsible for better sensitivity. Adsorption is a process in which surface particles are exposed partially to attract other particles at their sites and is a consequence of surface energy while desorption is a process in which there is a release of one substance to the other from the surface.[32,33] The comparative study of the material for electrical humidity sensing is depicted in Table 2.

For an ideal sensor, other parameters are also very important. The response time is defined as the time when the sensor achieved (10 to 95) %RH and recovery time is when the senor recovers its initial position (95 to 10) % RH. From Fig. 8 and Fig. 9, it is evident that the response and recovery at 100 Hz frequency of $(Ge_{11.5}Te_{12.5}Se_{67.5})_{100}$ are the 30s and 44s while for $(Ge_{11.5}Te_{12.5}Se_{67.5})_{90}Sb_{10}$ was found to be 28s and 34s respectively. The aging effect was also observed in Fig. 6(c) and Fig. 7(c) at 100 Hz frequency. After 1 week, 1 month, 2 months and 3 weeks, we can see that the aging can be significantly observed at low and mid humidity regime

Table 2. Sensitivity, ageing effect, repeatability, response and recovery time of $(Ge_{11.5}Se_{67.5}\ Te_{12.5})_{100}$ and $(Ge_{11.5}\ Se_{67.5}\ Te_{12.5})_{90}\ Sb_{10}$ chalcogenide sensing element.

Sensing element	Frequency	Average sensitivity MΩ/%RH	Repeatability	Response time	Recovery time
X=0	10^2 Hz	8.522	95.05%	30 s	44 s
X=10	10^2 Hz	9.280	96.25%	28 s	34 s

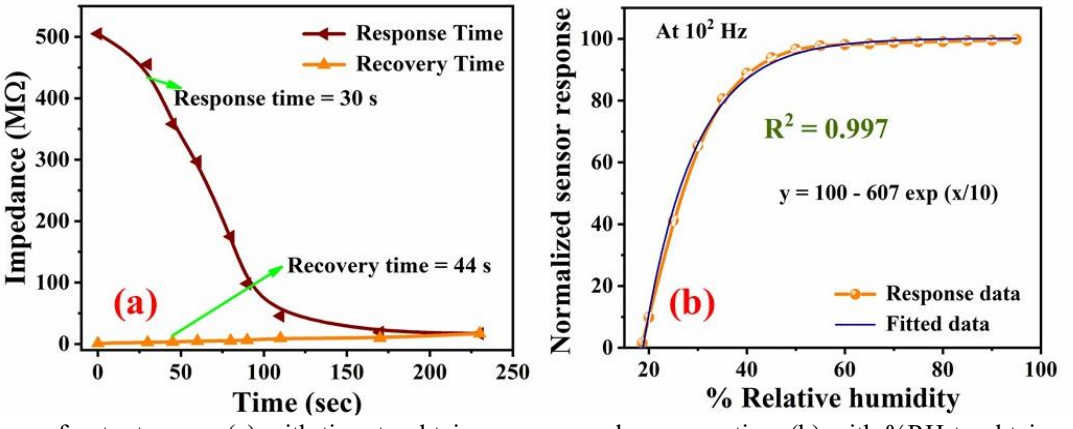

Fig. 8 Dependence of output power (a) with time to obtain response and recovery time (b) with %RH to obtain response data of $(Ge_{11.5}\ Te_{12.5}\ Se_{67.5})_{100}$ chalcogenide sensing element.

but it is found negligible at high relative humidity. The normalized sensor response is also calculated by using the formula:[34]

$$R = \frac{\Delta R}{R_0} \times 100 \quad (3)$$

where R is normalized response and ΔR is the response change in impedance between the dry atmosphere and different %RH. The value of R square was found as 0.997 for $(Ge_{11.5}Te_{12.5}\ Se_{67.5})_{100}$ and 0.990 for $(Ge_{11.5}Te_{12.5}Se_{67.5})_{90}\ Sb_{10}$ by using exponential fitting of the response data as shown in Fig. 8(b) and Fig. 9(b).

The prepared humidity sensors based on $(Ge_{11.5}Te_{12.5}Se_{67.5})_{100}$ and $(Ge_{11.5}Te_{12.5}Se_{67.5})_{90}Sb_{10}$ chalcogenide glassy alloys exhibited excellent sensing properties compared to other humidity sensors fabricated based on metal sulphides, oxide and other nanocomposites.[35-42] $(Ge_{11.5}Te_{12.5}Se_{67.5})_{100}$ and $(Ge_{11.5}Te_{12.5}Se_{67.5})_{90}Sb_{10}$ chalcogenide glassy alloys-based humidity sensors demonstrated better sensing properties and shows faster response and recovery times. Table 3 shows the sensing properties of previously studied materials for humidity sensing applications.

Table 3. Comparative study on the sensing performance of reported humidity sensors fabricated based on various material.

Materials	Sensitivity	Response and recovery time	Ref.
VS_2 nanosheets	0.70 MW/%RH	40/50 s	[35]
ZnO/TiO_2 core shell	0.89 MW/%RH	774.9/ 19.7 s	[36]
MoS_2 Quantum dots	2.21 MW/%RH	14/172 s	[37]
$Ni(NO_3)_2(AAm)4{\cdot}2H_2O$	0.37 MW/%RH	15.1/75.2 s	[38]
HEC/ PVDF	0.19 dB/%RH	-	[39]
Ag/TiO_2	0.92 MW/%RH	-	[40]
CZTS	0.10 MW/%RH	46/80 s	[41]
Hollow MoS_2 micro@nanospheres	0.32 nF/% RH	140 /80 s	[42]
$(Ge_{11.5}Se_{67.5}Te_{12.5})_{100}$ and $(Ge_{11.5}Se_{67.5}Te_{12.5})_{90}\ Sb_{10}$ glassy thin films	8.52 and 9.28 MW/%RH	30/44 s and 28/34 s	Present paper

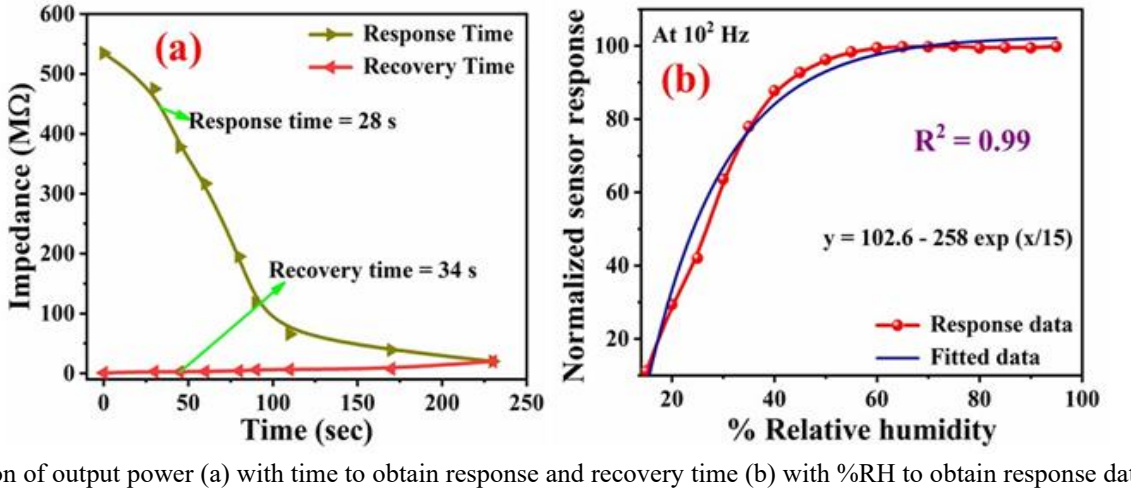

Fig. 9 Variation of output power (a) with time to obtain response and recovery time (b) with %RH to obtain response data of $(Ge_{11.5}\ Te_{12.5}\ Se_{67.5})_{90}\ Sb_{10}$ chalcogenide sensing element.

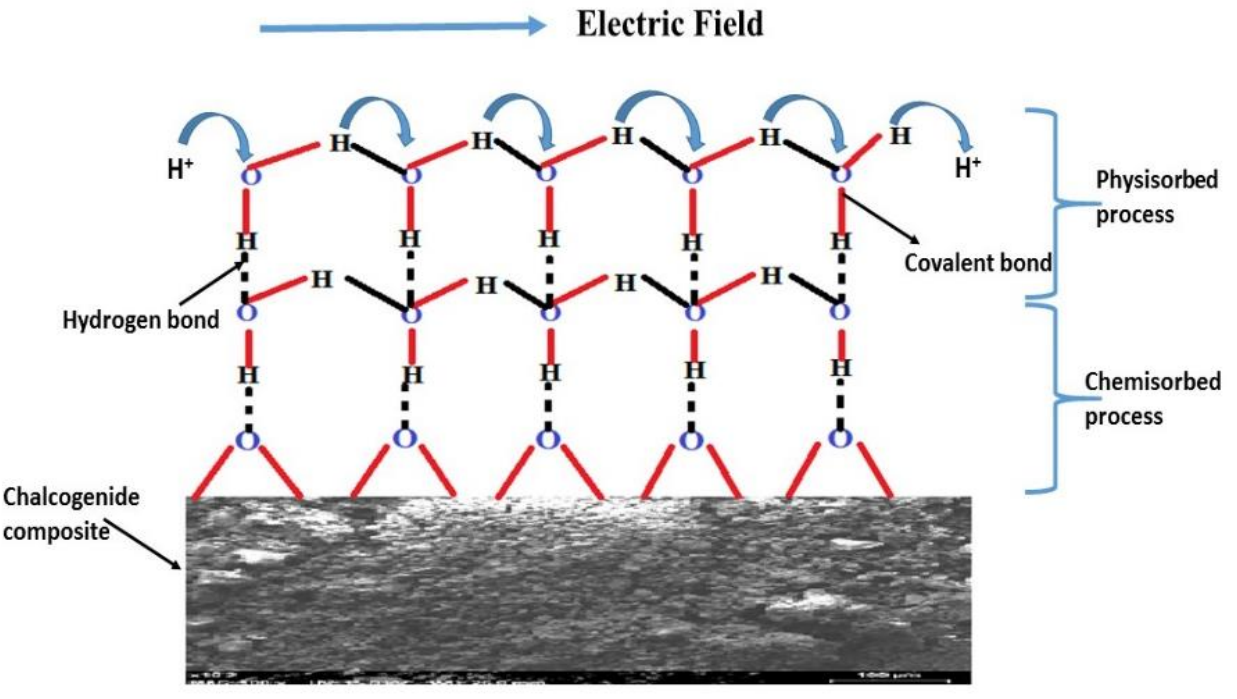

Fig. 10 Diagram explaining Grotthuss chain reaction in $(Ge_{11.5}\ Te_{12.5}\ Se_{67.5})_{100}$ and $(Ge_{11.5}\ Te_{12.5}\ Se_{67.5})_{90}\ Sb_{10}$ chalcogenide sensing material.

3.3. Humidity sensing mechanism

Water is a polar molecule, which easily interacts with the surface of the material. The humidity sensing mechanism is explained by the Grotthuss chain reaction as shown in Fig. 10. According to this phenomenon, initially, if the sensing film is free from water molecules *i.e.*, in a dry condition then no change was observed in impedance.[43,44] However, the water molecules begin to interact with the surface of the sensing material when humidity is revealed in the humidity control chamber, and it splits into two sections, *i.e.*, OH^- (hydroxyl) and H^+ ions (protons). When the metal (M^+) ions interact with a hydroxyl group then because of electrostatic force chemical bonding between the hydroxyl and protons ions, very high and the chemisorbed layer is formed. Protons have highly hopping power which connects to the surface side by side and H_3O^+ (hydronium) ions are formed and increase the conductivity of the sensing material which is responsible for sharp change in impedance while at low humidity exposure, the highest impedance value was found as shown in Fig. 10.[45,46]

The hydroxyl group was developed on the first physisorbed layer in the mid humidity region, which is possible due to weak Wander walls forces, so minor impedance changes were noticed and less sensitivity was observed in this region.[47] The second physically absorbed layer was then generated in the high humidity zone, and the capillary acts like condensation. So small proton ions are formed, resulting in the smallest impedance change and thus less sensitivity is observed in this area.[48,49]

4. Conclusion

In summary, high-performance impedance-based frequency dependent humidity sensors were prepared by two newly prepared chalcogenide glasses, *i.e.* $(Ge_{11.5}Te_{12.5}Se_{67.5})_{90}\ Sb_{10}$ and $(Ge_{11.5}Te_{12.5}Se_{67.5})_{100}$. The crystal structure and morphologies of the prepared chalcogenide glasses were confirmed by XRD and SEM analysis. The average sensitivity of prepared glasses was found to be 88.522 MΩ/%RH and 9.280 MΩ/%RH at a frequency of 100 Hz. The repeatability of fabricated sensors was measured as 95.05% and 96.25% for x= 0 and 10, respectively, which indicates that the sensitivity of sensing material enhances as the Sb concentration increases. The response and recovery time for $(Ge_{11.5}\ Te_{12.5}\ Se_{67.5})_{100}$ were 30s and 44s respectively while for $(Ge_{11.5}\ Te_{12.5}\ Se_{67.5})_{90}Sb_{10}$ it was calculated as 28 s and 34 s respectively. The aging effect can be significantly observed at low and mid humidity regime but it is found negligible at high relative humidity.

Acknowledgements

We are thankful to Central Instrument Facility (CIF), IIT (BHU), Varanasi for providing XRD facility.

Supporting information

Not applicable.

Conflict of interest

There are no conflicts to declare.

References

[1] C. Lee, G. Lee, *Sensor. Lett.*, 2005, **3**, 1-15, doi: 10.1166/sl.2005.001.

[2] S. M. M. Mousally, K. M. Al-Zaydi, C. Petrier, S. T. Arab, and M. S. Refat, *Sci. Adv. Mater.*, 2019, **11**, 1684–1691, doi:

10.1166/sam.2019.3612.
[3] C. C. Lin, Z. L. Tseng, and L. C. Chen, *J. Nano. Opto*., 2019**,** **14**, 729–733, doi: 10.1166/jno.2019.2516.
[4] F. D. Mei, Y. J. Li, C. Y. Hu, Z. H. Mei, and F. Ye, *Sci. Adv. Mater*., 2019, **11**, 1306–1314, doi: 10.1166/sam.2019.3512.
[5] S. Hussain, T. Liu, M. S. Javed, N. Aslame, W. Zeng, *Sensor. Actuat. B-Chem*, 2017, **239**, 1243–1250, doi: 10.1016/j.snb.2016.09.128.
[6] H. Wu, L. F. Meng, and W. G. Song, *Sci. Adv. Mater*., 2019**,** **11,** 1133–1139, doi: 10.1166/sam.2019.3547.
[7] S. Hussain, N. Aslam, X Y Yang, M.S. Javed , Z. Xu, M. Wang, G. Liu, G. Qiao, *Ceram. Int.*, 2018, **44**, 19624–19630, doi: 10.1016/j.ceramint.2018.07.212.
[8] R. Demir, S. Okur, M. Seker, *Ind. Eng. Chem. Res.*, 2012*,* **51**, 3309-3313, doi:10.1021/ie201509a.
[9] Q. Kuang, C. S. Lao, Z. L. Wang, Z. X. Zie, L. S. Zheng, *J. Am. Chem. Soc.*, 2007, **129**, 6070-6071, doi: 10.1021/ja070788m.
[10] S. Mishra, P. Jaiswal, P. Lohia and D. K. Dwivedi, *IEEE Xplore*, 2018**,** **1-5**, doi: 10.1109/UPCON.2018.8596828.
[11] A. Zakery, S. R. Elliott, *J. Non-Cryst. Solids*, 2003, **330**, 1-12, doi: 10.1016/j.jnoncrysol.2003.08.064.
[12] N. M. Santhosh, E. D. Mishina, A. Shestakova, and S. Thomas, *J. Nanoelectron. Optoe*., 2019, **14**, 1048–1055, doi: 10.1166/jno.2019.2621.
[13] J.A. Savage, *J. Non-Cryst. Solids*, 1982, **47**, 101-115, doi: 10.1016/0022-3093(82)90349-0.
[14] W. J. Yoo, J. K. Seo, *ISIEA*, 2009*,* **2**, 617-619, doi: 10.1109/ISIEA.2009.5356393.
[15] J. S. Sanghera, L. B. Shaw, I. D. Aggarwal, *Comp. Ren. Chim*., 2002, **5,** 873-883, doi: 10.1016/S1631-0748(02)01450-9.
[16] A. M. Andriesh, *J. Non-Cryst. Solids*., 1985, **7**, 1219-1228, doi: 10.1016/0022-3093(85)90878-6.
[17] M. Mitkova, P. Chen, M. Ailavajhala, D.P. Butt, D.A. Tenne, H. Barnaby, I.S. Esqueda, *J. Non-Cryst. Solids*, 2013, **377**, 195-199, doi: 10.1016/j.jnoncrysol.2012.12.031.
[18] A. K. Sharma, *J. Appl. Phys.*, 2013*,* **114**, 044701, doi: 10.1063/1.4816272.
[19] V.S. Vassilev, S.V. Boycheva. *Talanta*, 2005, **67**, 20-27, doi: 10.1016/j.talanta.2005.02.027.
[20] A. V. Legin, E. A. Bychkov, Y. G. Vlasov. *Sensor. Actuat. B-Chem*, 1995, **24**, 309-311, doi:10.1016/0925-4005(95)85067-8
[21] R. Tomova, G. Spasov, R. S. Topalova, A. Buroff, *Sensor. Actuat. B-Chem*, 2004, **103**, 277-283, doi: 10.1016/j.snb.2004.04.059.
[22] Yu. G. Mourzina, M. J. Schöning, J. Schubert, W. Zander, A. V. Legin, Yu. G. Vlasov, H. Lüth, *Anal. Chim. Acta*., 2001, **433**, 103-110, doi: 10.1016/S0003-2670(00)01384-2.
[23] A. E. Owen, *J. Non-Cryst. Solids*, 1990, **35-36**, 999-1004, doi: 10.1016/0022-3093(80)90331-2.
[24] K. Kolev, C. Popov, T. Petkova, *Sensor. Actuat. B-Chem*, 2009, **143**, 359-399, doi: 10.1016/j.snb.2009.08.016.
[25] P. K. Singh, D. K. Dwivedi, *Adv. Sci, Eng. Med.*, 2018**,** **10**, 670-674, doi: 10.1166/asem.2018.2212.
[26] S. Mishra, P. Lohia, D. K. Dwivedi, *Phy. B*, 2019, **572**, 81-87, doi: 10.1016/j.physb.2019.07.046.
[27] S. Mishra, P. Lohia, D. K. Dwivedi, *Infrared Phys. Technol.*, 2019, **100**, 109-116, doi: 10.1016/j.infrared.2019.05.001.
[28] P. Chaudhary, S. Sikarwar, B. C. Yadav, G. I. Dzhardimalieva, N. D. Golubeva, I. E. Uflyan, *Sensor. Actuat. A*, 2017, **263**, 415–422, doi: 10.1016/j.sna.2017.07.006.
[29] G. Uddin, M. Sajid, J. Ali, S. Wan, Y. Hoi, and K. Hyun, *Sensor. Actuat. B-Chem*, 2018**,** **266**, 354–363, doi: 10.1016/j.snb.2018.03.134.
[30] K. Tiwari and N. K. Pandey, *SPIE Digital Lib.*, 2015, **8549**, 8549161-6, doi: 10.1117/12.924796.
[31] M. Parthibavrman, V. Hariharan, C. Sekar, *Mater. Sci. Eng. C*, 2011, **31**, 840-844, doi: 10.1016/j.msec.2011.01.002.
[32] X. F. Song, Q. Qi, T. Zhang, C. Wang, *Sensor. Actuat. B-Chem*, 2009, **138**, 368-373, doi: 10.1016/j.snb.2009.02.027.
[33] V. Kumar, V. Chauhan, J. Ram, R. Gupta, S. Kumar, P. Chaudhary, B.C. Yadav, S. Ojha, I. Sulania, Rajesh Kumar, *Sr. Coat. Technol.*, 2020**,** **392**, 125768, doi: 10.1016/j.surfcoat.2020.125768
[34] R. Nohria, R. K. Khillan, Y. Su, R. Dikshit, Y. Lvov, and K. Varahramyan, *Sensor. Actuat. B-Chem*, 2006, **114**, 218–222, doi: 10.1016/j.snb.2005.04.034.
[35] J. Feng, L. Peng, C. Wu, X. Sun, S. Hu, C. Lin, J. Dai, J. Yang, Y. Xie, *Adv. Mater*., 2012, **24**, 1969-1974, doi: 10.1002/adma.201104681.
[36] L. Gu, K. Zheng, Y. Zhou, J. Li, X. Mo, G. R. Patzke and G. Chen, *Sensor. Actuat. B-Chem*, 2011, **159**, 1–7, doi: 10.1016/j.snb.2010.12.024.
[37] S. Yadav, P. Chaudhary, K. N. Uttam, A. Varma, M. Vashistha and B.C. Yadav, *Nanotechnology*, 2019, **30**, 295501-295512, doi: 10.1088/13616528/ab1569.
[38] P. Chaudhary, D. K. Maurya, S. Sikarwar, B. C. Yadav, G. I. Dzhardimalieva, R. Prakash, *Eur. Polym. J.*, 2019, **112**, 161-169, doi: 10.1016/j.eurpolymj.2018.12.032.
[39] B.C. Yadav, R.C. Yadav, S. Singh, P. K. Dwivedi, H. Ryu, S. Kang, *Opt. Laser Technol*., 2013, **49**, 68–74, doi: 10.1016/j.optlastec.2012.12.011.
[40] S. F. A. Z. Yusoff, C.S. Lim, S. R. Azzuhri, H. Ahmad, R. Zakaria, *Results Phys.*, 2018, **10**, 308-316, doi: 10.1016/j.rinp.2018.06.008.
[41] D. K. Maurya, S. Sikarwar, P. Chaudhary, S. Angaiah and B. C. Yadav, *IEEE Sensor. J.*, 2019**,** **19**, 2837-2845, doi: 10.1109/JSEN.2018.2890309.
[42] Y. Tan, K. Yu, T. Yang, Q. Zhang, W. Cong, H. Yin, Z. Zhang Z, Chenb Y and Zhua, *J. Mater. Chem. C*, 2014, **2**, 5422–3, doi: 10.1039/C4TC00423J.
[43] B. C. Yadav, S. Sikarwar, R. Yadav, P. Chaudhary, G. I. Dzhardimalieva, N. D. Golubeva, *J. Mater. Sci.: Mater. Electron.*, 2018, **29**, 7770–7777, doi: 10.1007/s10854-018-8774-0.
[44] D. Zhang, Y. Sun, P. Li, and Y. Zhang, *ACS Appl. Mater. Inter.*, 2016, **8**, 14142−14149, doi: 10.1021/acsami.6b02206.
[45] B. Collignon, P. N. M. Hoang, S. Picaud, J. C. Rayez, *Chem. Phys. Lett.*, 2005**,** **406**, 430-435, doi: 10.1016/j.cplett.2005.03.026.
[46] X. J. Chen, J. Zhang, Z. L. Wang, Q. Yan, S. C. Hui, *Sensor. Actuat. B-Chem*, 2011**,** **156**, 631-636, doi:

10.1016/j.snb.2011.02.009.
[47] Y. Wang, S. Park, J. T. W. Yeow, A. Langner, F. Muller, *Sensor. Actuat. B-Chem*, 2010, **149**, 136-142, doi: 10.1016/j.snb.2010.06.010.
[48] D. Zhag, H. Chang, P. Li, R. Liu, Q. Xue, *Sensor. Actuat. B-Chem*, 2016, **225**, 233-240, doi: 1016/j.snb.2015.11.024.
[49] D. Zhang, J. Tong, B. Xia, *Sensor. Actuat. B-Chem*, 2014, **197**, 66-72, doi: 10.1016/j.snb.2014.02.078.

Author information

Dr. Surabhi Mishra *has completed her Ph.D. in physics in 2021 from Madan Mohan Malaviya University of Technology, Gorakhpur. Her research area of interest includes the investigations on chalcogenide thin films, humidity sensors and in other sensing applications, carbon nano tubes, quantum dots.*

Ms. Priyanka Chaudhary *is pursuing Ph.D. in BBA (Central) University, Lucknow. She has received her B.Sc. and M.Sc., M.Phil. (Gold Medalist) degrees in 2012, 2014 and 2016, respectively from University of Lucknow, Lucknow and BBA (Central) University, Lucknow. Her research area of interest includes the investigations on nano metallopolymers and quantum dots with their humidity and gas sensing applications.*

Prof. (Dr.) B. C. Yadav *is Professor in the Department of Physics, School of Physical & Decision Sciences in the Babasaheb Bhimrao Ambedkar University, Lucknow. He is the recipient of prestigious Young Scientist Award-2005 instituted by the State Council of Science and Technology. His current interests of research include the synthesis of metal oxides nanoparticles, metallopolymers, etc., characterizations and their applications as physical and chemical sensors.*

Prof. (Dr.) Ahmad Umar *received his Ph.D. in semiconductor and chemical engineering from Chonbuk National University, South Korea. He worked as a research scientist in Brain Korea 21, Centre for Future Energy Materials and Devices, Chonbuk National University, South Korea, in 2007–2008. Afterwards, he joined the Department of Chemistry in Najran University, Najran, Saudi Arabia. He is a distinguished professor of chemistry and served as deputy director of the Promising Centre for Sensors and Electronic Devices (PCSED), Najran University, Najran, Saudi Arabia. Professor Ahmad Umar is specialized in 'semiconductor nanotechnology', which includes growth, properties and their various high technological applications, for instance, gas, chemicals and biosensors, optoelectronic and electronic devices, field effect transistors (FETs), nanostructure-based energy-harvesting devices, such as solar cells, Li-ion batteries, super-capacitors, semiconductor nanomaterial- based environmental remediation, and so on. He is also specialized in the modern analytical and spectroscopic techniques used for the characterizations and applications of semiconductor nanomaterials. He contributed to the world of science by editing world's first handbook series on Metal Oxide Nanostructures and Their Applications (5-volume set, 3500 printed pages, www.aspbs.com/mona) and handbook series on Encyclopedia of Semiconductor Nanotechnology (7-volume set; www.aspbs.com/esn), both published by American Scientific Publishers (www.aspbs.com). He has published more than 600 research papers in reputed journal with h-index of 75 and i10-index of 377 with total citations of 20221 (According to Google scholar).*

Dr. Pooja Lohia *is assistant professor in Department of Electronics and Communication Engineering in the Madan Mohan Malaviya University of Technology, Gorakhpur. Her current research interests include chalcogenide glasses, sensors, waveguide sensors, solar cells etc. She has published more than 50 research articles in the reputed journal.*

Prof. (Dr.) D. K. Dwivedi *is professor in Department of Physics and Material Science in the Madan Mohan Malaviya University of Technology, Gorakhpur. He is also Dean of Faculty Affairs in Madan Mohan Malaviya University of Technology, Gorakhpur. He has guided 6 Ph.D. scholar and published more than 200 articles. His current research interest includes amorphous semiconductor, sensor, solar cell, optical fiber sensor, SPR sensors etc.*

Publisher's Note: Engineered Science Publisher remains neutral with regard to jurisdictional claims in published maps and institutional affiliations.